J. Shanghai Jiaotong Univ. (Sci.), 2011, 16(6): 1-4
DOI: 10.1007/s12204-009-0501-3

Sensitivity Analysis of Thermal Properties on Numerical Simulation Results of Quenching Process

ZHOU Zhi-fang (周志方), *GU Jian-feng** (顾剑锋), *WANG Xiao-yan* (王晓燕), *PAN Jian-sheng* (潘健生)
(Shanghai Key Laboratory of Materials Laser Processing and Modification, School of Materials Science and Engineering, Shanghai Jiaotong University, Shanghai 200240, China)

Abstract: A three-factor three-level orthogonal test project has been designed based on the numerical simulation of a Jominy quenching process. Then the data scattering effects of thermal conductivity and enthalpy of tested steel, as well as the heat exchange coefficients of the cooling media, on the results have been studied. The results can be used as a reference for choosing the input thermal parameter in finite element simulation of quenching, and for evaluating the simulation results.
Key words: finite element simulation, orthogonal test method, thermal input parameters, quenching
CLC number: TG 156.31 **Document code:** A

0 Introduction

As an effective method, the finite element simulation has been more and more popular in the studying of the quenching process design, as well as the evaluation of the properties of the production quenched[1]. The accuracy of the quenching simulation depends on the accuracy of the input numerical parameters. However, some of the input parameters, like the heat exchange coefficient of the quenching media and the properties of the quenched steel in the very high temperature, are difficult to get accurately. Thus it is hard to avoid scattering for the input numerical parameters used in the quenching simulation.

In this paper, the scattering effects of three kinds of input parameters on the Jominy quenching simulation results have been discussed by a three-factor three-level orthogonal test method. These input parameters are the heat exchange coefficients of the water and air, and the enthalpy and thermal conductivity of the quenched steel.

1 Numerical Simulation

1.1 Finite Element Model

A quenching process of a non-standard Jominy specimen made of GCr15 steel has been simulated by the finite element method, the size of which is ∅25 mm × 100 mm. It is an axis-symmetry structure, so only the rotational surface has been used to simulate, and the model is meshed into 500 elements and 561 nodes, as shown in Fig. 1. The specimen was quenched at the bottom surface by water, and the others were cooled by air. The heat exchange coefficients of the water and air ($K_{\rm w}, K_{\rm a}$) are shown in Fig. 2. The enthalpy (h) and thermal conductivity (κ) of GCr15 are shown in Figs. 3 and 4. The rest parameters of GCr15 can be referred to Ref. [2].

The heat conduction of quenching process was governed by the Fourier law[3]. The volume fraction of

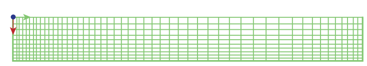

Fig. 1 Element of the Jominy specimen

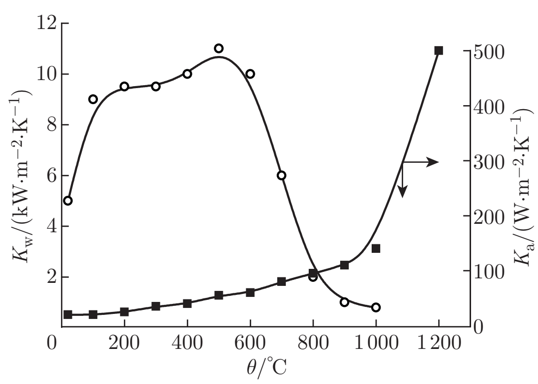

Fig. 2 Heat exchange coefficients of water and air

Received date: 2010-10-15
Foundation item: the Major Scientific Research Project of Shanghai science & Technology Commission (No. 08DZ1100302) and the National Basic Research Program (973) of China (No. 2011CB706600)
***E-mail:** gujf@sjtu.edu.cn

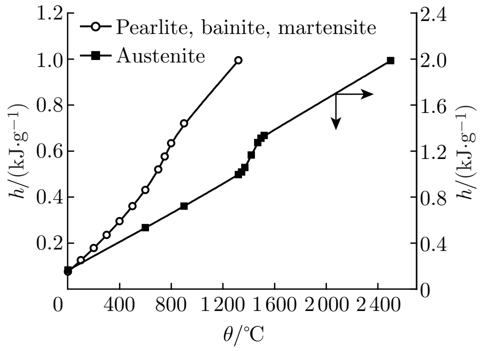

Fig. 3 Enthalpy values of GCr15

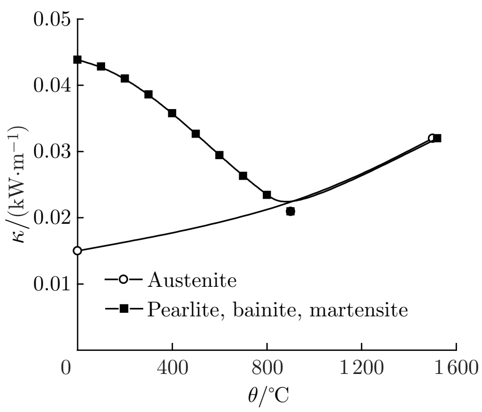

Fig. 4 Thermal conductivity values of GCr15

pearlite and bainite transformed was calculated by the Johnson-Mehl-Avrami equation[4-7]. The volume fraction of martensite transformed was calculated by the Koistinen-Marburger equation[8]. With an increased iteration method, the elastic and plastic strain, thermal strain, and transformation strain were all concerned[9-10] during the quenching process. Then the Vicker hardness HV of the specimen was gained by summed method.

1.2 Orthogonal Test Project

A three-factor three-level orthogonal test project has been designed to study the data scattering effects of the input parameters on the simulation results. They are heat exchange coefficient (K) of cooling media, as well as the enthalpy (h) and thermal conductivity (κ) of GCr15. Parameters K, h and κ are three factors in the project. Volume fraction of martensite, quenched strength and hardness are compared by three kinds of values: D_{50} which is the quenched depth corresponding to the 50% volume fraction of martensite, $\sigma_{\max}$ which is the maximum quenched strength, and d_{HV400} which is the depth above Vicker hardness HV400. In this paper, values of D_{50}, $\sigma_{\max}$ and d_{HV400} corresponded to the original input parameter, K, h and κ are denoted by subscript 1, the results corresponded to the above input parameter, with a plus 10% scattering are denoted by subscript 2, and those of minus 10% scattering are denoted by subscript 3. These parameters are three levels in orthogonal test method, as shown in Table 1.

Table 1 Orthogonal test project and result

Test number	Orthogonal project			D_{50}/mm	$\sigma_{\max}$/MPa	d_{HV400}/mm
1	K_2	κ_2	h_3	16.7	176	66.3
2	K_2	κ_3	h_1	15.9	201	55.4
3	K_2	κ_1	h_2	16.5	181	56.0
4	K_3	κ_2	h_1	15.5	203	53.6
5	K_3	κ_3	h_2	14.5	228	46.9
6	K_3	κ_1	h_3	14.7	214	52.2
7	K_1	κ_2	h_2	16.6	184	55.2
8	K_1	κ_3	h_3	14.9	214	52.8
9	K_1	κ_1	h_1	15.6	201	54.6

2 Results and Discussion

2.1 Simulation and Discussion

The original microstructure of the specimen is uniform austenite, after quenching the microstructure in the specimen has changed. And the microstructure volume fraction along the symmetric axis is shown in Fig. 5. At the quenching surface, they are mixture of 90% (volume fraction) martensite and 10% (volume fraction) residual austenite. The volume fraction of martensite and residual austenite decreases from 8 mm depth and almost disappears at 32 mm depth. Meanwhile the volume fraction of bainite increases from zero to near 100% and then begins to decrease too at 40 mm depth, until at 68 mm depth arrives at near zero. On the contrary, the volume fraction of pearlite increases from zero to near 100% at the same time. Among them, martensite is the most important for quenching process, so the volume fraction of martensite is the first result analyzed in the orthogonal test project, as shown in Table 1.

The Von Mises equivalent stress along the symmetric axis is shown in Fig. 6. It is a wavy curve. The biggest

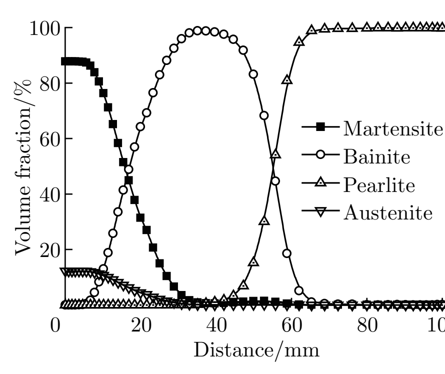

Fig. 5 Phase volume contents along the symmetric axis

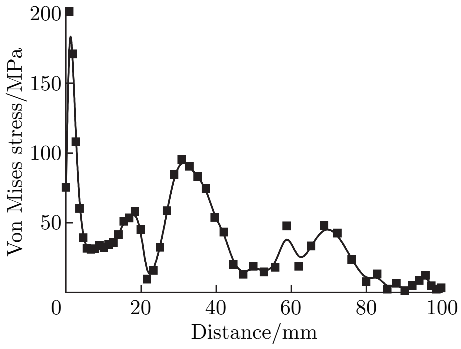

Fig. 6 Von Mises stress along the symmetric axis

peak corresponds to the depth that bainite transformation begins to happen, and the volume fraction of martensite and residual austenite begins to decrease. The second peak occurs at about 32 mm that corresponds to the end of the martensite transformation, and residual austenite occurs; the volume fraction of bainite begins to be short stable also. The third peak of Von Mises stress occurs at 68 mm that corresponds to the end of the bainite transformation, and the volume fraction of pearlite begins to be stable. In general, the maximum Von Mises equivalent stress $\sigma_{\max}$ is concerned. Thus it is the second result analyzed in the orthogonal test project, as shown in Table 1.

Vicker hardness HV along the symmetric axis decreases with three platforms, as shown in Fig. 7. The first platform is close to the quenching surface, which corresponds to the maximum martensite volume fraction. The second platform occurs within depth from about 32 to 48 mm, which corresponds to the region of the maximum bainite volume fraction. The last platform begins from about 68 mm to the end, which corresponds to the austenite decomposed to pearlite totally. The hardening depth is also an important index to evaluate the harden ability, so d_{HV400} is regarded as the third result analyzed in the orthogonal test project.

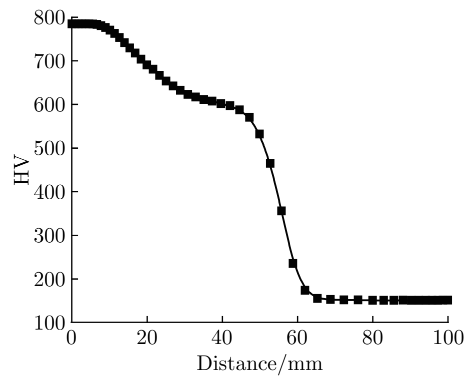

Fig. 7 Vicker hardness HV along the symmetric axis

2.2 Orthogonal Test and Discussion

The maximum of D_{50}, d_{HV400} and the minimum $\sigma_{\max}$ values occur at the combination of (K_2, κ_2, h_3), and the minimum of D_{50}, d_{HV400} and maximum $\sigma_{\max}$ values occur at the combination of (K_3, κ_3, h_2), as shown in Table 1. It is thoughtful that D_{50} and d_{HV400} have the same tendency, because the martensite gives the biggest contribution for the hardness. However, the $\sigma_{\max}$ value changes following the different rule. It can be considered that the $\sigma_{\max}$ value depends stronger on the heat transfer of test steel and heat exchange boundary condition than on the inner heat source due to the change of enthalpy.

According to the orthogonal test method, T_1 line values in Table 2 mean the sum of results corresponding to all combination that include K_1, κ_1 and h_1, and they

Table 2 Orthogonal test results and analysis

	D_{50}/mm			$\sigma_{\max}$/MPa			d_{HV400}/mm		
	K	κ	h	K	κ	h	K	κ	h
T_1	47.1	46.8	47	599	596	605	162.6	162.8	163.6
T_2	49.1	48.8	47.6	558	563	593	177.7	175.1	158.1
T_3	44.7	45.3	46.3	645	643	604	152.7	155.1	171.3
t_1	15.7	15.6	15.7	199.7	198.7	201.7	54.2	54.3	54.5
t_2	16.4	16.3	15.9	186.0	187.7	197.7	59.2	58.4	52.7
t_3	14.9	15.1	15.4	215.0	214.3	201.3	50.9	51.7	51.7
R^*	1.5	1.2	0.5	29.0	26.6	4.0	8.3	6.7	2.8
Optimum level (max $\{t_1, t_2, t_3\}$)	K_2	κ_2	h_2	K_3	κ_3	h_1	K_2	κ_2	h_1
Primary	(K_2, κ_2, h_2)			(K_3, κ_3, h_1)			(K_2, κ_2, h_1)		

Note: $R^* = \max\{t_1, t_2, t_3\} - \min\{t_1, t_2, t_3\}$

are all results corresponding to level 1; t_1 line values mean the average of T_1, and they equal to T_1 divided by 3; T_2, T_3, t_2 and t_3 line values have the similar definition. After the orthogonal test in Table 2, it is more clear that K is the primary factor which affects all the D_{50}, $\sigma_{\max}$ and $d_{\mathrm{HV}400}$. Parameter h has the weakest effect on all these results; κ is between K and h. While maximum values of these three kinds of results are wanted, it is advised to choose combination of (K_2, κ_2, h_2), (K_3, κ_3, h_1) and (K_2, κ_2, h_1), separately. Or we can find which parameter is the key parameter while we want to adjust these properties by this method.

3 Conclusion

The Von Mises equivalent stress along the rotational axis has three apparent peaks, and the Vicker hardness HV along the rotational axis has three platforms, both of which correspond significantly to the point to gain the maximum bainite volume fraction and the point which bainite starts decompose in the specimen.

Even though heat exchange coefficient of cooling media, the enthalpy and thermal conductivity of GCr15 have the same scattering of 10%, they have quite different effects on the simulation results. According to the results of D_{50}, $\sigma_{\max}$ and $d_{\mathrm{HV}400}$, heat exchange coefficient of cooling media has the strongest effect, meanwhile enthalpy has the weakest effect on all these results. The combination of (K_2, κ_2, h_2), (K_3, κ_3, h_1) and (K_2, κ_2, h_1) will give the maximum results of D_{50}, $\sigma_{\max}$ and $d_{\mathrm{HV}400}$ separately.

References

[1] Yao Xin, Gu Jian-feng, Hu Ming-juan. 3D temperature and microstructure modeling of large-scale P20 steel mould quenching in different processes [J]. *Heat Treatment of Metals*, 2003, **28**(7): 33-37 (in Chinese).

[2] Yao Xin. The application of computer simulation on the quenching of large-sized mould blocks and bearing steel [D]. Shanghai: School of Materials Science and Engineering, Shanghai Jiaotong University, 2003 (in Chinese).

[3] Tao Wen-quan. Heat transfer [M]. Xi'an: Northwestern Polytechnical University Press, 2006 (in Chinese).

[4] Johnson W A, Mehl R F. Reaction kinetics in process of nucleation and growth [J]. *Transactions on AIME*, 1939, **135**: 416-458.

[5] Avrami M. Kinetics of phase change. I. General theory [J]. *Journal of Chemical Physics*, 1939, **7**(12): 1103-1112.

[6] Avrami M. Kinetics of phase change. II. Transformation-time relations for random distribution of nuclei [J]. *Journal of Chemical Physics*, 1940, **8**(2): 212-224.

[7] Avrami M. Kinetics of phase change. III. Granulation, phase change and microstructure [J]. *Journal of Chemical Physics*, 1941, **9**(2): 177-184.

[8] Koistinen D P, Marburger R E. A general equation prescribing extend of austenite-martensite transformation in pure Fe-C alloys and plain carbon steels [J]. *Acta Metallurgica*, 1959, **7**(1): 59-60.

[9] Leblond J B, Mottet G, Devaux J C. A theoretical and numerical approach to the plastic behaviour of steels during phase transformations. I. Derivation of general relations [J]. *Journal of the Mechanics and Physics of Solids*, 1986, **34**(4): 395-409.

[10] Leblond J B, Mottet G, Devaux J C. A theoretical and numerical approach to the plastic behavior of steels during phase transformations. II. Study of classical plasticity for ideal plastic phases [J]. *Journal of the Mechanics and Physics of Solids*, 1986, **34**(4): 411-432.